


Identification of the Differential Expression Profiles of Serum and Tissue Proteins During Rat Hepatocarcinogenesis

Technology in Cancer Research & Treatment
 Volume 17: 1–13
 © The Author(s) 2018
 Reprints and permission:
sagepub.com/journalsPermissions.nav
 DOI: 10.1177/1533034618756785
journals.sagepub.com/home/tct


Xia Sheng, PhD¹, Tao Huang, MS², Jianmin Qin, PhD, MD^{2,3},
 Lin Yang, MS², Zhong-qiu Sa, MS², and Qi Li, PhD, MD⁴

Abstract

The pathogenesis of hepatocellular carcinoma is complex and not fully known yet. This study aims to screen and identify the differentially expressed proteins in peripheral blood and liver tissue samples from rat hepatocellular carcinoma and to further clarify the pathogenesis and discover the specific tumor markers and molecular targets of hepatocellular carcinoma. The hepatocellular carcinoma model of Wistar rats were induced by chemical carcinogen. The serum and liver tissue samples were obtained after induction for 2, 4, 8, 14, 18, and 21 weeks. The results showed that the clusterin (IPI00198667), heat shock protein a8 (IPI00208205), and N-myc downstream-regulated gene-2 (IPI00382069) being closely related to hepatocarcinogenesis were eventually identified from the 30 different proteins. As the time progressed, the serum levels of clusterin and heat shock protein a8 increased gradually during induced liver cancer in rats. However, the serum N-myc downstream-regulated gene 2 level in induced liver cancer in rats underwent biphasic changes, and the serum N-myc downstream-regulated gene 2 level decreased at the 8th week, increased at the 14th week, and then decreased significantly. Statistical difference occurred in protein expression of clusterin and heat shock protein a8 in liver tissues at the different time points. In the liver tissues, the N-myc downstream-regulated gene 2 level decreased gradually at the 8th week, increased gradually at the 14th week, and then decreased significantly after 14 weeks. The study demonstrated that heat shock protein a8, clusterin, and N-myc downstream-regulated gene 2 participated in the process of abnormal cell division, proliferation, and carcinogenesis of liver cells during hepatocarcinogenesis.

Keywords

hepatocellular carcinoma (HCC), occurrence, proteomics, diagnosis, target therapy

Abbreviations

HCC, hepatocellular carcinoma; HSPa8, heat shock protein a8; NDRG2, N-Myc downstream-regulated gene-2; SDS, sodium dodecyl sulfate; PBS, phosphate-buffered saline; LSC, liver stem cell; mRNA, messenger RNA; DENA, diethylnitrosamine; SDS-PAGE, sodium dodecyl sulfate-polyacrylamide gel electrophoresis; LSD, least-significant difference.

Received: August 23, 2017; Revised: November 9, 2017; Accepted: December 21, 2017.

Introduction

Hepatocellular carcinoma (HCC) is one of the common malignant tumors. Each year about 750 000 patients have HCC worldwide, and 600 000 patients die of liver cancer. The mortality of HCC ranks second in the malignant tumors, and it seriously threatens health of humans.¹ Fifty-five percent of new HCC cases occur in China every year, and mortality due to HCC ranks second among various cancers in China and is only second to lung cancer.² The pathogenesis of HCC is complex and related to environmental and genetic factors. It involves

¹ Department of pathology, Affiliated to the Third Hospital, Second Military Medical University, Shanghai, P.R. China

² Department of General Surgery, Putuo Hospital, Shanghai University of Traditional Chinese Medicine, Shanghai, P.R. China

³ Department of general surgery, Affiliated to the Third Hospital, Second Military Medical University, Shanghai, P.R. China

⁴ Department of Medical Oncology, Shuguang Hospital, Shanghai University of Traditional Chinese Medicine, Shanghai, P.R. China

Corresponding Author:

Jianmin Qin, PhD, MD, Department of General Surgery, Affiliated to the Third Hospital, Second Military Medical University, 700, North Moyu Road, Jiangding district 201805, Shanghai, P.R. China.
 Email: jianminqin@yahoo.com



hepatitis B or (and) C virus infection, aflatoxin-contaminated food or water, carcinogens such as nitrosamines, butter yellow, chloroform, parasitic infections, and so on. The occurrence, hyperplasia, carcinogenesis, and metastasis of HCC involve in multiple genes and proteins. It is a more complicated process involving multiple factors and steps synergy. Proteomics is performed to obtain the peptide and protein sequences of serum, tissues, or cells using protein mass spectrometry.³ The 2-dimensional gel electrophoresis map and protein database were analyzed and constructed to screen and identify the differential proteins to establish the proteomic database by bioinformatics.⁴ Using SWISS-PROT and TrEMBL databases, the differential protein peaks were compared to proteins with equal length or mass charge ratio to obtain the length range of proteins, then search differential protein peaks that are nearest, and identify related proteins.⁵ Differential proteomics can compare the number, location, and modification of protein expression of tissues and cells in normal and pathological states and find the specific proteins associated with the pathological status or disease. Differential proteomics is of great value in studying the pathogenesis of malignant tumors, searching for the diagnostic markers of malignant tumors, and screening the metastasis-associated proteins and molecular-targeted drugs.⁶ The proteomics and its related technology are used to study the protein expression profiles of HCC occurrence and development; it is not only beneficial for screening the tumor-specific markers of HCC but also for determining the therapeutic targets for HCC, improving the early diagnosis and therapeutic effect of HCC. Paradis et al⁷ analyzed the serum of 82 patients with liver cirrhosis (44 cases of liver cancer among the patients) by surface-enhanced laser desorption/ionization-time of flight-mass spectrometry. The results showed that 30 differential protein peaks associated with HCC and cirrhosis were identified. The 6 peaks of the highest score were used to diagnose HCC, and the diagnostic accordance rate was over 90%. Among them, 3 peaks were the C-terminal part of the V10 fragment of vitronectin, which were considered as potential markers for early screening and diagnosis of HCC. Hu et al⁸ compared the proteins of hepatitis B virus-infected HCC tissues and adjacent non-HCC tissues in 9 groups and identified the 222 differentially expressed proteins. Further studies indicated that reducing the expression of glucose-6-phosphate dehydrogenase could reduce the metastasis and recurrence rate of HCC. This present study aims to screen and identify the differentially expressed proteins in peripheral blood and liver tissue samples from rat HCC induced by diethyl nitrosamine using 2-dimensional gel electrophoresis and tandem time-of-flight mass spectrometry techniques at different time points. The level of the differential proteins in peripheral blood and liver tissue is detected using enzyme-linked immunosorbent assay (ELISA) and Western blotting techniques; the location of the differential proteins in liver tissues is detected using immunohistochemical technique. This study has important biological significance for further understanding the pathogenesis of HCC and finding specific tumor markers and molecular targets of HCC.

Materials and Methods

Reagents

Diethyl nitrosamine, Proteo-Prep Immunoaffinity Albumin and IgG Depletion Kit, thiourea, dithiothreitol, iodine acetamide, sodium thiosulfate, and 2-dimensional gel electrophoresis standard protein were purchased from Sigma Company. Solid phase pH gradient dry strip (IPC strip pH 3-10 L, and 24 cm), interpublic buffer (pH : 3-10), ampholytes (pharmalyte, pH 3-10), low-molecular-weight protein, protein silver dye kits, urea, propylene phthalein amine, double propylene phthalein methylene amine, glycerin, glycine, nonidet P-40, 3-hydroxymethyl aminomethane, 3-[(3-bravery acyl amino propyl) dimethyl amine] propyl sulfonate, phenylmethylsulfonyl fluoride, Triton X-100, sodium dodecyl sulfate (SDS), EDTA, and filter column were purchased from Amershma Bioseiences Company. IPGhor isoelectric focusing (GE Healthcare), DALT-6 sodium dodecyl sulfate-polyacrylamide gel electrophoresis (SDS-PAGE) electrophoresis apparatus, ImageScanner scanner, ImageMaster 2d Platinum 7.0 analysis software were purchased from GE Healthcare Company. ABI4800 tandem time-of-flight mass spectrometer (MALDI-TOF/TOF) is purchased from America ABI Co LTD. The primary and second antibodies of clusterin, NDRG2, and HSPa8 are purchased from Santa Cruz biotechnology Co, Ltd.

Rats and Grouping

Six-week-old male Wistar rats, weighing from 140 to 160 g, were provided by the Shanghai Laboratory Animal Center (Chinese academy of sciences, license SCXK Shanghai 2003-0003). All rats were quarantined for 1 week before the start of the experiment. They were housed in an animal facility maintained on a 12-hour light-dark cycle, at a constant temperature of $23^{\circ}\text{C} \pm 1^{\circ}\text{C}$ and a relative humidity of $44\% \pm 5\%$ and were given free access to tap water and food. The rats were randomly divided into the control group and the induced cancer group according to the experiment design. Each group had 10 Wistar rats. The experimental protocols were reviewed and approved by the Committee of Ethics on Animal Experiments of the animal facility, and all the animal work procedures were approved by the Institutional Animal Care and Use Committee of Shanghai University of Traditional Chinese Medicine.

Establishment of Rat HCC Model

The rats in the induced cancer group were fed with standard fodder and diethylnitrosamine (DNA) water (DNA content, 0.05 g/L) for 2 weeks; then DNA water (DNA content, 0.05 g/L) was changed into DNA water (DNA content, 0.1 g/L) for 8 weeks, and later DNA water (DNA content, 0.1 g/L) was changed into normal drinking water after 10 weeks.³⁷ The Wistar rats in the control group were fed with standard fodder and normal drinking water. The experimental protocols were reviewed and approved by the Committee of Ethics on Animal Experiments of the animal facility, and all the

animal work procedures were approved by the Institutional Animal Care and Use Committee of Shanghai University of Traditional Chinese Medicine.

Acquirement of Serum and Tissue Samples

After all rats were killed by ether, 2 mL venous blood from inferior vena cava, liver tissues, and tumor tissues were, respectively, were acquired from Wistar rats in the control group and the induced cancer group before and after induction for 2, 4, 8, 14, 18, and 21 weeks. Ten rats were killed at the indicated time. Liver and tumor tissues were, respectively, dehydrated at different concentration of ethanol and embedded with paraffin, and then 4- μ m slice was prepared to be stained with hematoxylin–eosin dye for pathological examination. The samples of serum, liver tissues, and tumor tissues were, respectively, frozen at is -80°C for protein mass spectrometry analysis and identification.

Histopathological Examination of Liver Tissues in Induced Liver Cancer

Paraffin slices of liver tissue in each group at the different time points were processed with xylene clearing, ethanol dehydration, hematoxylin–eosin staining, ethanol dehydration, xylene clearing, and neutral gum mounting step by step, and then the pathological changes were observed under a microscope.

Removal of Serum High-Abundant Proteins

Filter column with balance fluid was centrifuged at the speed of 8000 rpm for 10 seconds at room temprature, and the balance fluid was removed from filter column. After the procedure was repeated 3 times, 40 μL of balance fluid and 60 μL of serum in each group were added into the upper part of filter column, incubated at 20°C for 10 minutes, and then centrifuged at 10 000 rpm for 60 seconds. The filtered fluid was added into the upper part of filter column, incubated at 20°C for 10 minutes, and then centrifuged at 10 000 rpm for 60 seconds. A total of 125 μL of balance fluid was added into the upper part of filter column, centrifuged at 10 000 rpm for 60 seconds, and then the filter fluid was, respectively, frozen at -80°C for protein mass spectrometry analysis. Serum protein concentration was determined by Bradford method.³⁸

Preparation of Liver and Tumor Tissue Protein Samples

A total of 0.1 g frozen liver or tumor tissue was fully grinded, 2 mL tissue lytic fluid was added into tissue, and then was incubated at 36°C for 1 hour. The mixture was centrifuged at 15 000 rpm for 15 minutes at room temprature, the supernatant was extracted from mixture, and then the supernatant was centrifuged 15 000 rpm for 15 minutes at room temperature again to remove impurities. The supernatant was frozen at -80°C for protein mass spectrometry analysis. Tissue protein concentration was determined by Bradford method.

Isoelectric Focusing

Serum or tissue protein sample of 450 μL with a protein content of 400 μg was slowly added into focusing slot; gel strip was slowly put into protein solution without bubble formation in the case of gel surface downward, 2 mL covered oil was slowly added on the surface of gel strip, and then the cover lid of focusing slot was added. The parameter of isoelectric focusing was set at 20°C and maximum current of 50 μA per strip. The procedure of isoelectric focusing was done successively at 50V \times 12 hours (step), 500V \times 1 hour (step), 1000V \times 1 hour (step), 1000 to 8000 V \times 1 hour(gradient), 8000 V \times 10 hours (step), and 500 V \times 10 hours (step).

Gel Strip Balance and SDS-PAGE

Gel strip in each group was taken out of focusing slot after isoelectric focusing was completed. The covered oil and residual protein solution on the gel surface were sucked out, and the gel strip was added 10 mL balance fluid 1 for 15 minutes, and then the gel strip was put into 10 mL balance fluid 2 for 15 minutes. The balanced gel strip was incubated in the SDS-PAGE electrophoretic buffer solution for 30 seconds, then added to the surface of SDS-PAGE gel, and then the gel strip and SDS-PAGE gel were placed the electrophoretic tank and electrophoresed at 15°C . The electrophoresis was done continuously at 100V \times 1 hour, 200 V, and until bromophenol blue ran out of the gel.

Gel Staining

After electrophoresis, the gel was rinsed with ultrapure water for 1 minute, fixed with fixation solution for 30 minutes, sensitized with sensitizing solution for 30 minutes, then rinsed with ultrapure water for 5 minutes for 3 times, stained with silver dye solution for 30 minutes, and then rinsed with ultrapure water for 1 minute twice. The gel was washed with developing solution until the strip was clear, stopped with stop bath solution for 10 minutes, and then rinsed with ultrapure water for 5 minutes thrice. The gel was stored in 1% acetic acid.

Gel Imaging and Image Analysis

The stained gel at the indicated time was scanned in a grayscale manner at the optical density value of 300 dpi using an Image Scanner. The scanned images were, respectively, analyzed using ImageMaster 2D Platinum 7.0 software. Compared to 0 time point, the protein expression at the indicated time was quantified in case of gel protein point detection, image background subtraction, protein point gray value standardization, and protein point matching between different gels. The *t*-test was performed among 3 groups of different time points with fold change being more than 2 times or less than 0.5 times. *P* value $<$.05 was considered to be statistical significant difference between protein points. The statistical difference in protein points were, respectively, obtained from the gel subjected to mass spectrometry.

Protein Enzymolysis

Every protein gel point was added to a test tube, rinsed with ultrapure water twice, destained with silver destaining solution for 10 minutes, and rinsed with deionized water twice. Imbibitional solution was added to the test tube for 5 minutes, removed, then dehydrated solution 1 was added to the test tube to dehydrate for 5 minutes, and removed; dehydrated solution 2 was added into the test tube to dehydrate for 5 minutes and removed. Zymolytic working solution of 10 μL was added to the test tube to imbibe for 30 minutes, and then 20 μL zymolytic covering solution was added into test tube to enzymolyse at 37°C for 12 hours. The supernatant was removed, and 50 μL protein extractive solution was added to the test tube in the water bath at 37°C for 30 minutes, centrifuged at 5000 rpm for 5 minutes, and supernatant was removed. All supernatant was lyophilized to be analyzed by mass spectrometry.

Protein Mass Spectrometry

Lyophilized powder of every protein gel point was dissolved in 5 μL of 0.1% trifluoroacetic acid (TFA) solution and mixed with α -cyano-4-hydroxy cinnamic acid saturated solution containing 50% acetonitrile and 1%TFA in 1:1 proportion. Mixed sample of 1 μL was taken out to identify the point target of mass spectrum by ABI4800 MALDI-TOF/TOF Mass Spectrometer. Positive ion mode and automatic data mode were used to collect data. The mass spectrum scanning range of peptide mass fingerprinting was from 800 to 3500 Da, and the 10 peaks of maximum strength were selected to be secondary mass spectrometry. The primary and secondary mass spectrum data were integrated to analyze and identify the proteins by the GPS3.6 (Applied Biosystems) and Mascot2.1 (Matrix Science) softwares. The processing and control images of 2-dimensional electrophoresis were, respectively, compared, and the statistical difference in protein points were analyzed by mass spectrometry with the fold change being more than 2 times or less than 0.5 times; P value was $<.05$. Rattus was database, enzyme was trypsin, maximum omissive cut site was 1, fixed modification was carbamidomethyl (C), variable modification was oxidation (M), MS tolerance was 0.15 Da, MS/MS tolerance was 0.25 Da, and protein score CI% being greater than 95 was regarded as successful identification.

Assay for Serum Expression of Clusterin, NDRG2, and HSPa8 Using ELISA Technique

Serum sample of 100 μL at different time points in each group was added into each well of culture plate and incubated at 37°C for 2 hours. After liquid of each well was removed, 200 μL 5% fetal bovine serum was added into each well to block the antigens at 37°C for 40 minutes. After liquid of each well was removed, 100 μL working solution A was added into each well; then, the primary antibodies including anti-clusterin antibody(1:200), anti-NDRG2 antibody(1:200), anti-HSPa8 antibody(1:200), and anti- β -actin antibody(1:200) were,

respectively, added into each well and incubated at 37°C for 1 hour. After liquid of each well was removed, it was washed with washing solution for 3 times for 6 minutes, and then 100 μL of working solution B was added into each well and incubated at 37°C for 30 minutes. After liquid of each well was removed, washed with washing solution 5 times for 10 minutes, 90 μL trimethylhexamethylenediamine substrate solution was added into each well, incubated at 37°C for 15 to 25 minutes (finish time according by the actual colour reaction), and then 50 μL terminated solution was added into each well; absorbance of each well was measured using enzyme standard instrument at 450 nm wavelength.

Assay for Protein Expression of Clusterin, NDRG2, and HSPa8 in Liver Tissue With Western Blotting Technique

A total of 12.5 μL 5 \times SDS loading buffer was added into 50 μg protein sample at different time points in each group, denatured at 100°C for 10 minutes, and cooled in ice bath. Protein marker, control samples, and protein samples at different time points in each group were, respectively, added into 10% SDS-PAGE gel hole, electrophoretic buffer solution was slowly added into electrophoretic tank, and gel electrophoresis was performed at 80 V for 20 minutes and then at 120 V until the bromophenol blue was near the bottom of gel. Gel was taken out and placed on the cellulose acetate membrane and protein electrotransfer was performed by Electrotransfer Apparatus at 350 mA for 2 hours, and then the cellulose acetate membrane was immersed into the blocking solution containing 5% skimmed milk powder and gently shaken for 1 hour. After the blocking solution was removed, the cellulose acetate membrane was, respectively, placed in 5 mL primary antibody solution including anti-clusterin antibody (1:200), anti-NDRG2 antibody (1:200), anti-HSPa8 antibody (1:200), and anti- β -actin antibody (1:200) overnight at 4°C. The membranes were rinsed with PBST buffer solution at room temperature for 15 minutes thrice. After the primary antibody solution was removed, 5 mL of the secondary antibody solution was added and incubated at room temperature for 1 hour with a horseradish peroxidase-conjugated secondary antibody (1:1000). The membranes were rinsed with PBST buffer solution at room temperature for 15 minutes 3 times again. The each band was, respectively, scanned with the Odyssey near-infrared scanners, the gray value of each band was analyzed with Quantity One software, the relative quantity of target protein expression was expressed with the gray value of each band and the gray value of β -actin ratio. Three independent blots were analyzed for each protein.

Detection of Location of Expression of Clusterin, NDRG2, and HSPa8 in Liver Tissues Using Immunohistochemistry Technique

After the paraffin slices of liver tissue in each group at the different time points were, respectively, processed with

xylene clearing and gradient ethanol dehydration, the paraffin slices were, respectively, incubated in 3% hydrogen peroxide solution at room temperature for 10 minutes and rinsed with 0.01 mol/L phosphate-buffered saline (PBS) solution for 5 minutes 3 times. Proteinase K solution of 50 μ L (dilution 20 μ g/mL) was, respectively, added on the tissue slice to digest proteins at 37°C for 20 minutes and then rinsed with double distilled water for 5 minutes 3 times. The paraffin slices were placed in citrate buffer solution (pH 6.0) and boiled for 10 minutes, placed at room temperature for 20 minutes, and then blocked with animal serum for 30 minutes. After the serum was removed, the primary antibodies including anti-clusterin antibody (1:100), anti-NDRG2 antibody (1:100), and anti-HSPa8 antibody (1:100) were, respectively, added on to the tissue slices and left overnight at 4°C. The tissue slices were rinsed with 0.01 mol/L PBS at room temperature for 3 minutes 3 times, the primary antibody solution was removed, and then the secondary antibody solution was added on the tissue slices at room temperature for 30 minutes. Then, the tissue slices were rinsed with 0.01 mol/L PBS at room temperature for 3 minutes 3 times and placed in the avidin–biotin–peroxidase complex solution (Vector, Cat: PK-6100) at room temperature for 30 minutes, then rinsed with 0.01 mol/L PBS at room temperature for 3 minutes 3 times, colorated with diaminobenzidine reagent about 2 minutes, rinsed with water, and redyed with hematoxylin. The paraffin slices were processed with xylene clearing and gradient ethanol dehydration, sealed with neutral gum, and then observed under light microscope.

Tissue cells with brown particles in nuclei were identified as positive cells that expressed the target protein and were counted at 200 \times magnification. Three visual fields were randomly selected in each slice, and the average of 3 visual fields was used for statistical analysis.

Statistical Analysis

Statistical analysis was performed using the Statistical Package for Social Sciences, version 17.0, statistics software (SPSSInc, Cabit Information Technology Co. Ltd, Shanghai). The mean was expressed as $\bar{x} \pm S$. Analysis of variance was used to compare difference between the groups at the different time points. Levene test was used for variance homogeneity, and the level of Levene test was $\alpha = 0.05$. Least-significant difference test was adopted when variances were homoscedastic. The approximate *F* test Welch method was employed and Dunnett T3 method was used between the groups when variances were not homoscedastic. $P < .05$ indicated significant differences.

Results

Morphological and Histopathological Changes in Liver Tissues During Induced Liver Cancer

The volume of liver lobe became swollen and large at the eighth week, and many white nodules occurred on the liver

surface. The volume of liver lobe became obviously swollen and larger at the 14th week, and large tumor lesions occurred at the liver surface. Many tumor lesions occurred in liver tissues at the 18th 21st week, and there were a lot of tumor vessels and necrotic lesions on the surface of tumor tissues. Rat hepatocytes underwent hypertrophy, degeneration, necrosis, fibrosis, and nucleolus atypia within 2 to 4 weeks during induced liver cancer (Figure 1B and D). Hepatocytes underwent obviously nucleolus atypia, structure disorder, and cancer focus formation within 8 weeks. Hepatocytes had pathologic mitosis, bigger nucleolus, and typical pathological manifestations of liver cancer within 14 to 21 weeks (Figure 1F and H).

Screening of Serum Differential Proteins During Induced Liver Cancer in Rats

The primary and secondary mass spectrum data from the protein spots of serum 2-dimensional electrophoresis were integrated for analysis. Fifteen differential proteins were screened by comparing the mass spectrometric data between the control group and the induced cancer group (Figure 2 and Table 1).

Screening of Differential Proteins of Liver Tissues During Induced Liver Cancer in Rats

The primary and secondary mass spectrum data from the protein spots of tissue 2-dimensional electrophoresis were integrated for analysis. Fifteen differential proteins were screened by comparing the mass spectrometric data between the control group and the induced cancer group at the different time points (Figure 3 and Table 2).

Identification of Differential Proteins of Serum and Liver Tissues

Three differential proteins closely related to hepatocarcinogenesis were identified from 30 different proteins of serum and liver tissues with protein score CI% being >95 . The 3 identified proteins were, respectively, clusterin (IPI00198667), N-Myc downstream-regulated gene-2 (NDRG2; IPI00382069), and heat shock protein a8 (HSPa8; IPI00208205).

Serum Expression of Clusterin, NDRG2, and HSPa8 During Induced Liver Cancer in Rats

As the time progressed, the serum levels of clusterin and HSPa8 in induced liver cancer in rats increased gradually (Figures 4 and 5). However, the serum NDRG2 level in induced liver cancer in rats underwent biphasic changes, and the serum NDRG2 level decreased at the 8th week, increased at the 14th week, and then decreased significantly (Figure 6).

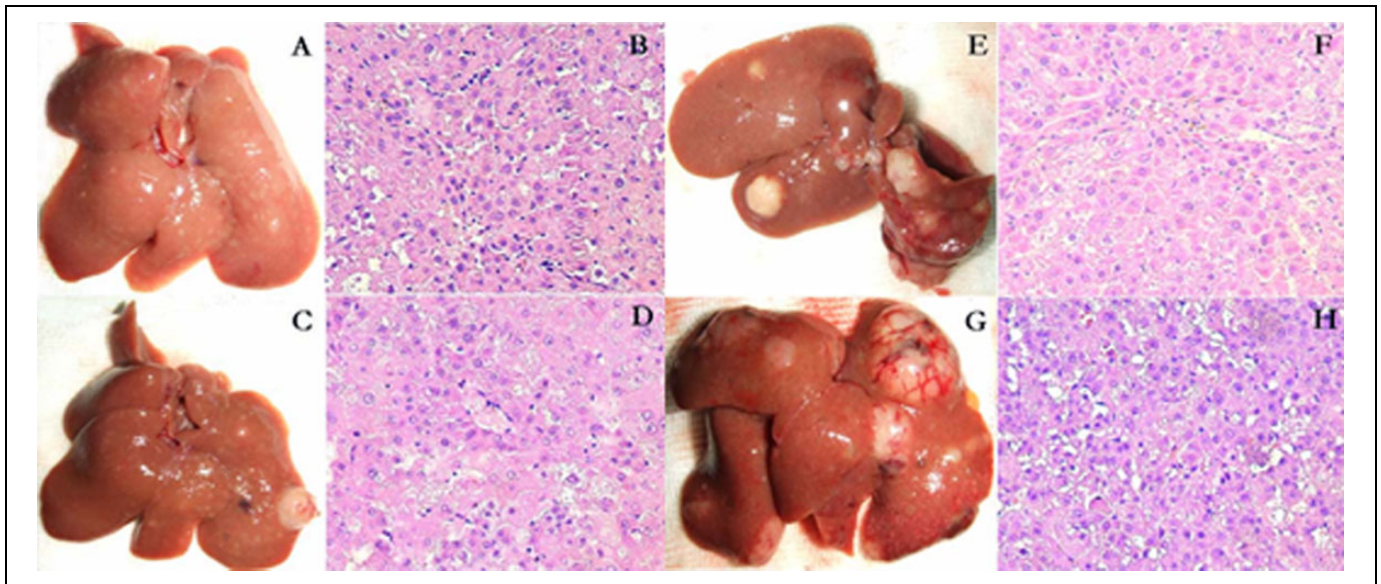


Figure 1. Morphological changes and tissue pathology of liver tissues during induced liver cancer in rats. A, The volume of liver lobe became swollen and large at the eighth week, and the liver surface had many white nodules. B, Hepatocytes occurred obviously nucleolus atypia, structure disorder, and canceration (original magnification HE $\times 200$). C, The volume of liver lobe became obviously swollen and larger at the 14th week, and the liver surface showed large tumor lesions. D, Hepatocytes had a lot of large nucleolus, and some hepatocytes became cancer cells (original magnification HE $\times 200$). E, Many tumor lesions occurred in liver tissues at the 18th week. F, Liver tissues had structure disorder and a lot of cancer cells and became typical pathological manifestations of hepatocellular carcinoma (original magnification HE $\times 200$). G, Many tumor lesions occurred in liver tissues at the 21st week, and there were a lot of tumor vessels and necrotic lesions on the surface of tumor tissues. H, Hepatocytes had typical nucleolus atypia, structure disorder, and intracytoplasmic vacuoles degeneration. The histopathological manifestations were typical hepatocellular carcinoma (original magnification HE $\times 200$).

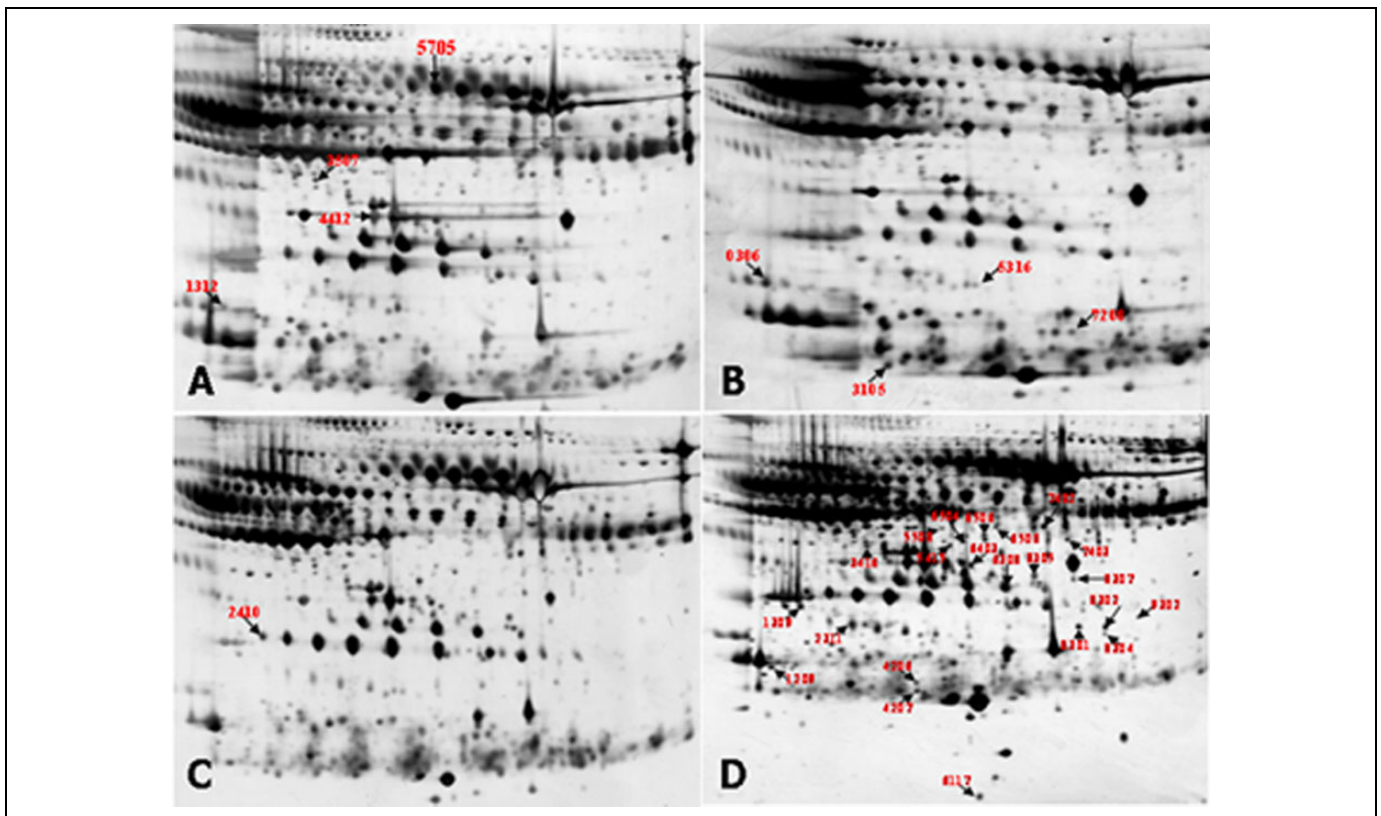


Figure 2. Serum 2-dimensional gel electrophoresis at the different time points during induced liver cancer in rats. A, Serum 2-dimensional gel electrophoresis in normal control rats. B, Serum 2-dimensional gel electrophoresis at the fourth week during induced liver cancer in rats. C, Serum 2-dimensional gel electrophoresis at the 14th week during induced liver cancer in rats. D, Serum 2-dimensional gel electrophoresis at the 21st week during induced liver cancer in rats.

Table 1. Screened Serum Protein Profiles at Different Time Points During Induced Liver Cancer in Rats.

Gel Point Number	MS Targets Number	Accession No	Protein Name	Protein Score	CI%
SSP 5415		J9	IPI00480639 C3 complement C3(fragment)	336	100
SSP 4412		J19	IPI00480639 C3 complement C3 (fragment)	571	100
SSP 7311		J6	IPI00382202 Hp isoform 2 of haptoglobin	418	100
SSP 5106		J8	IPI00382202 Hp isoform 2 of haptoglobin	378	100
SSP 2410		J12	IPI00382202 Hp isoform 2 of haptoglobin	435	100
SSP 4104		L8	IPI00201561 Prdx2 oeroxiredoxin-2	460	100
SSP 1210		J7	IPI00191502 Psma5 proteasome subunit α type-5	551	100
SSP 8123		J15	IPI00876581 Rbp4 retinol-binding protein 4	489	100
SSP 2411		J16	IPI00324272 Apoa4 apolipoprotein A-IV	504	100
SSP 4206		K10	IPI00197703 Apoa1 apolipoprotein A-I	330	100
SSP 8309		K15	IPI00191737 Alb serum albumin	356	100
SSP 6117		L22	IPI00400456 LOC259246 rat (wistar)	384	100
SSP 8307		L5	IPI00782222 Pzp 167 kDa protein	452	100
SSP 8305		K1	IPI00782222 Pzp 167 kDa protein	440	100
SSP 5316		K16	IPI00198667 Clu clusterin	547	100

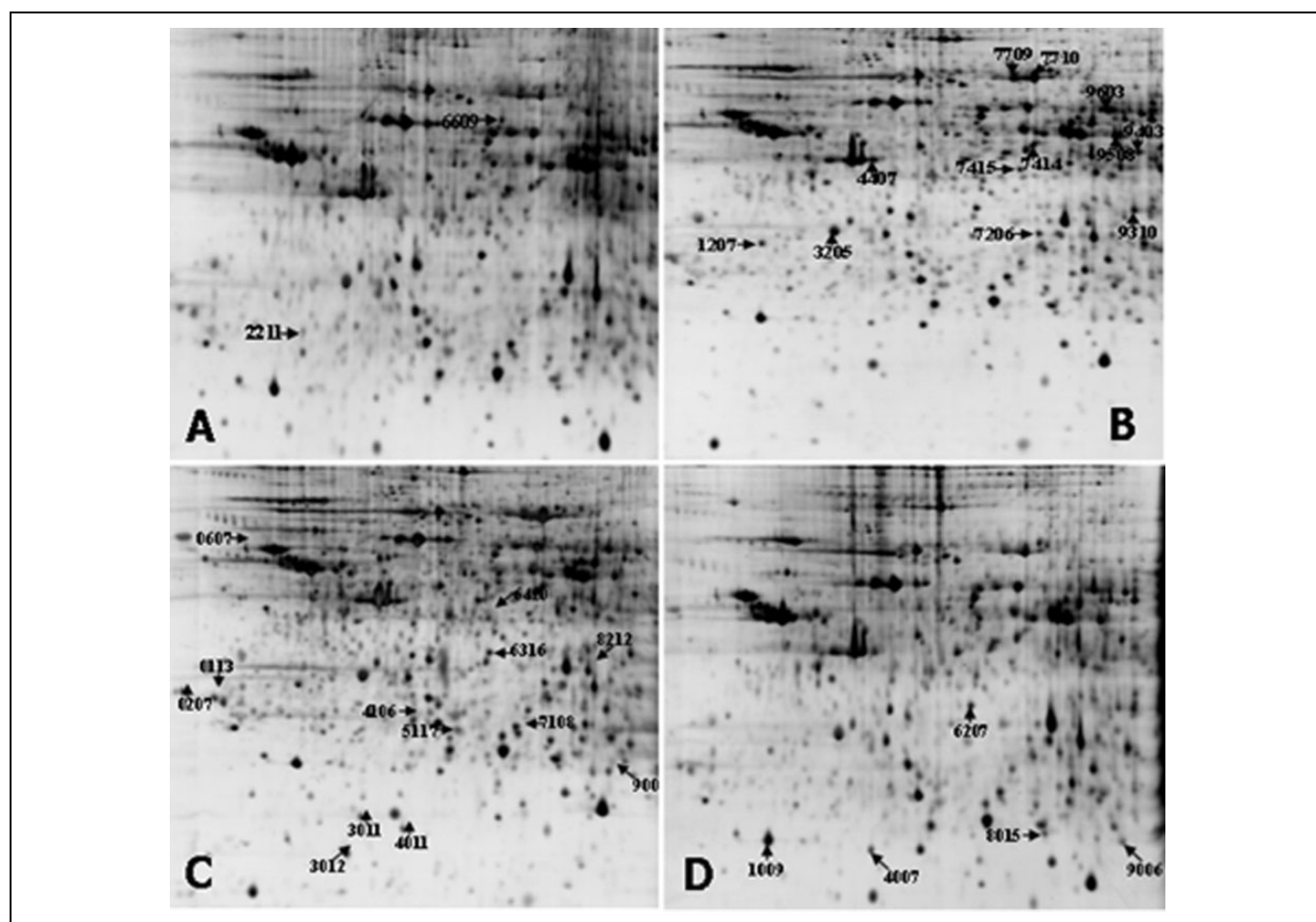


Figure 3. Two-dimensional gel electrophoresis of liver tissues at the different time points during induced liver cancer in rats. A, Two-dimensional gel electrophoresis of liver tissue at the fourth week during induced liver cancer in rats. B, Two-dimensional gel electrophoresis of liver tissue at the 14th week during induced liver cancer in rats. C, Two-dimensional gel electrophoresis of liver tissue at the 21st week during induced liver cancer in rats. D, Two-dimensional gel electrophoresis of paraneoplastic liver tissue at the 21st week during induced liver cancer in rats.

Table 2. Screened Protein Profiles of Liver Tissues at Different Time Points During Induced Liver Cancer in Rats.

Gel Point Number	MS Targets Number	Accession No	Protein Name	Protein Score	C. I. %
SSP 3012	M8	IPI00231229	Gstp1 glutathione S-transferase P	523	100
SSP 1207	M19	IPI00471889	Anxa5 annexin A5	601	100
SSP 6316	N3	IPI00190377	Taldo1 transaldolase	257	100
SSP 9603	N4	IPI00231064	Aldh3a1 aldehyde dehydrogenase, dimeric NADP-preferring	430	100
SSP 9007	N9	IPI00231229	Gstp1 glutathione S-transferase P	518	100
SSP 8212	N24	IPI00206092	Akr1b8 aldose reductase-like protein	432	100
SSP 0607	O6	IPI00734561	Tra1 isoform 2 of endoplasmic	496	100
SSP 9310	O9	IPI00325765	Akr7a2 aflatoxin B1 aldehyde reductase member 2	258	100
SSP 7206	O16	IPI00213610	Cry11 lambda-crystallin homolog	559	100
SSP 6010	M11	IPI00231963	Ddt D-dopachrome decarboxylase	312	100
SSP 0209	N6	IPI00382069	NdrG2 isoform 1 of Protein NDRG2	335	100
SSP 2005	N7	IPI00192246	Cox5a cytochrome c oxidase subunit 5A, mitochondrial	390	100
SSP 7505	O2	IPI00551702	Dlst dihydrolipoylysine-residue succinyltransferase component of 2-oxoglutarate dehydrogenase complex	372	100
SSP 5714	O18	IPI00208205	Hspa8 heat shock cognate 71 kDa protein	718	100
SSP 5205	M24	IPI00765011	LOC295810 similar to actin, cytoplasmic 2	441	100

Abbreviations: Hspa8, heat shock protein a8; NDRG2, N-Myc downstream-regulated gene-2

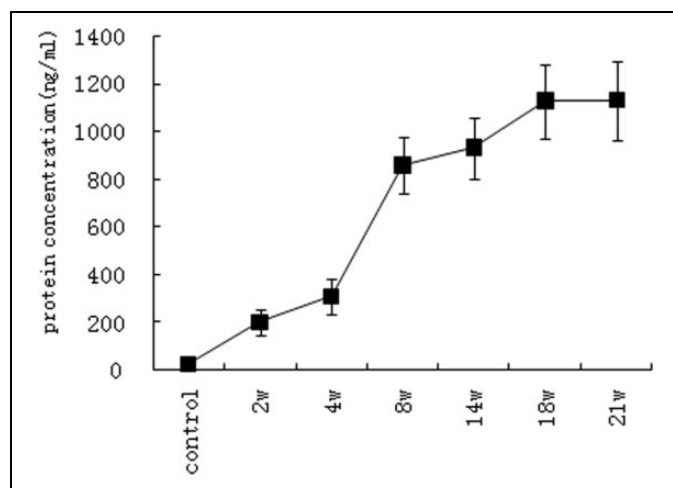


Figure 4. The serum level of clusterin during induced liver cancer in rats. The curve chart showed that as the time prolonged, the serum level of clusterin increased gradually compared to the control group.

Protein Expression of Clusterin, NDRG2, and HSPa8 in Liver Tissues During Induced Liver Cancer in Rats

The protein expression of clusterin and HSPa8 in liver tissues at the different time points didn't have a statistical difference between the control group and the induced cancer group ($P > .05$). The NDRG2 level in liver tissues decreased gradually at the 8th week, increased gradually at the 14th week, and then decreased significantly after 14 weeks ($P < .05$), which was consistent with the serum level of NDRG2 (Figure 7).

Location and Expression of Clusterin, NDRG2, and HSPa8 in Liver Tissues During Induced Liver Cancer in Rats

The expression of clusterin in the cytoplasm of hepatocytes was weakly positive in the liver parenchyma at the second week

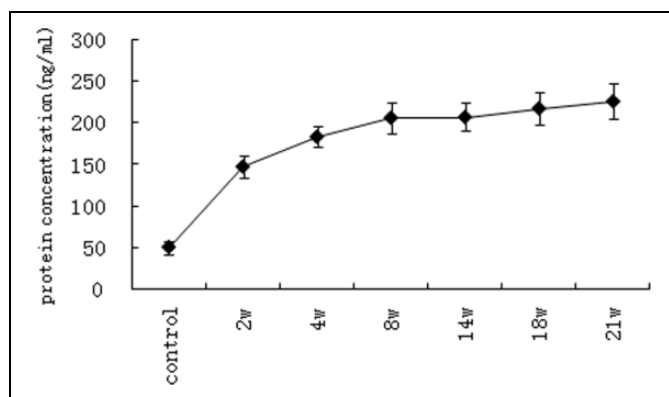


Figure 5. The serum level of heat shock protein a8 (HSPa8) during induced liver cancer in rats. The curve chart showed that as the time prolonged, the serum level of HSPa8 increased gradually compared to the control group.

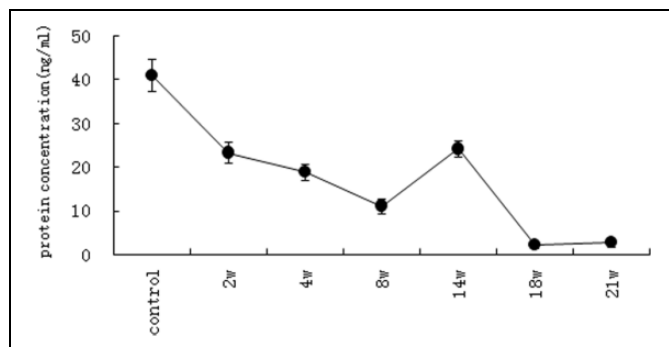


Figure 6. The serum level of N-myc downstream-regulated gene-2 (NDRG2) during induced liver cancer in rats. The curve chart showed that as the time prolonged, the serum level of NDRG2 underwent biphasic changes, and the serum NDRG2 level decreased gradually from 2 to 8 weeks, increased gradually from 8 to 14 weeks, and then decreased significantly after 14 weeks.

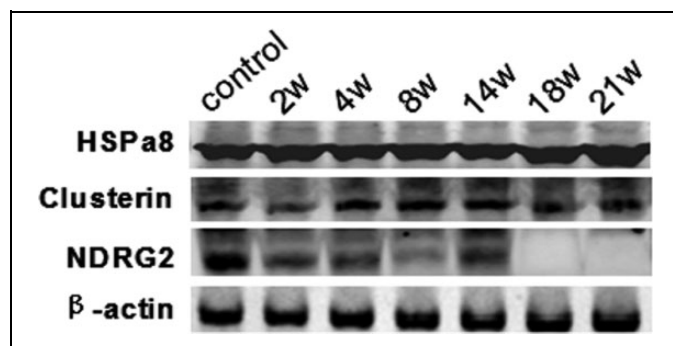


Figure 7. The protein expression of clusterin and heat shock protein a8 (HSPa8) in liver tissues at the different time points didn't show statistical difference. The N-myc downstream-regulated gene-2 (NDRG2) level in liver tissues decreased gradually at the eighth week, increased gradually at the 14th week, and then decreased significantly after 14 weeks; this indicated that the NDRG2 expression showed biphasic changes in liver tissues at the different time points.

(Figure 8A). Expression of clusterin in hepatocytes was located in the cytoplasm around the portal area at the fourth week (Figure 8B). The clusterin expression in hepatocytes increased significantly at the 8th week ($P < .05$; Figure 8C), decreased significantly at the 14th and 18th week ($P < .05$; Figure 8D and E), and then increased significantly at the 21st week ($P < .05$; Figure 8F).

The expression of HSPa8 in the cytoplasm of hepatocytes occurred in liver parenchyma at the second week (Figure 9A). The expression of HSPa8 in the cytoplasm of hepatocytes increased gradually in liver parenchyma from the 4th week to 21st week (Figure 9B-F).

The expression of NDRG2 in the cytoplasm and nucleus of mesenchymal cells occurred around portal area at the second week (Figure 10A). The expression of NDRG2 in cytoplasm and nucleus of hepatocytes increased gradually in liver parenchyma from the fourth to eighth week (Figure 10B and C). The expression of NDRG2 in cytoplasm of hepatocytes decreased gradually in liver parenchyma after the 14th week (Figure 10D-F).

Discussion

The deregulation of the cell cycle results in the abnormal cell proliferation and apoptosis, and it plays an important role in the occurrence and development of tumor. Alaiya et al⁹ analyzed the differences in protein expression between the cancerous tissue and normal liver tissue by proteomic and immunohistochemical techniques; the results showed that the aldose reductase-like protein, whose relative molecular mass and isoelectric point were, respectively, 35 000 Da and 74, was expressed in the precancerous lesions and liver cancer tissue; however, there was no expression in the normal liver tissue. It indicated that these changes might be closely related to the pathogenesis of liver cancer.⁹ Poon et al¹⁰ screened 250 different proteins in serum samples from patients with liver cancer, cirrhosis, and healthy persons using the proteomic technique.

Different proteins demonstrated the specificity of the liver cancer proteome and were better markers for early diagnosis of HCC. We established the rat HCC model induced by diethylnitrosamine agent; the proteome in the serum and liver tissue samples was screened and identified by 2-dimensional gel electrophoresis and tandem time-of-flight mass spectrometry, and the results showed that 15 serum differential proteins and 15 tissue differential proteins were, respectively, screened according to protein score $CI\% > 95$. The 3 differential proteins closely related to hepatocarcinogenesis were eventually identified from the 30 different proteins. The 3 differential proteins were clusterin (IPI00198667), HSPa8 (IPI00208205), and NDRG2 (IPI00382069), respectively.

Clusterin is a kind of heterologous dimer-sulfated glycoprotein common in the cytoplasm of normal cells and can stabilize the cell membrane and regulate the intercellular matrix interaction and differentiation, cell cycle, transformation, apoptosis, movement, oxidative stress, DNA repair, adhesion, membrane regeneration, and circulation of epithelial cell.¹¹ Qian et al¹² found that the positive rate of clusterin in liver cancer tissue was 82.93%, and the expression of clusterin in liver cirrhosis and normal liver tissues was negative or weakly positive. The degree of tumor differentiation was lower, the clusterin level in liver cancer tissue was higher, and it indicated that clusterin could promote the proliferation, metastasis, and invasion of liver cancer cells. Recent studies found that serum clusterin significantly increased in patients with HCC and decreased in patients with cirrhosis and chronic hepatitis. Moreover, serum clusterin significantly increased in patients with HCC being poorly differentiated, portal vein, and lymph node invasion. The optimal threshold of serum clusterin level was 128 $\mu\text{g}/\text{mL}$, and the sensitivity and specificity of predicting HCC was, respectively, 90% and 89%, if serum clusterin level was more than 128 $\mu\text{g}/\text{mL}$. It could also be used as a potential indicator for predicting the development and metastasis of HCC.^{13,14} Our current study found that serum clusterin level gradually increased with the prolongation of time during hepatocarcinogenesis in rats. Expression of clusterin in the cytoplasm of hepatocytes was positive around the portal area at the fourth week. Expression of clusterin in the cytoplasm of hepatocytes was strongly positive around the portal area at the eighth week. However, the clusterin expression in the cytoplasm of hepatocytes was weakly positive in liver parenchyma at the 14th and 18th week. The clusterin expression in the cytoplasm of hepatocytes was strongly positive in liver parenchyma at the 21st week. It indicated that clusterin played a positive role in inducing cancer in normal liver cells by promoting the abnormal proliferation of normal liver cells.

Heat shock cognate protein a8, also known as HSP70, is a main intracellular molecular chaperone and has lower expression in normal cells.^{15,16} The increase in expression of HSPa8 induced by the malignant transformation of cells results in the abnormal expression of HSPa8 in tumor cells. Through interaction with c-myc, c-fos, p53, and their protein products, HSPa8 can regulate the proliferation, apoptosis, differentiation of cells, tumor resistance, and immune in the case of

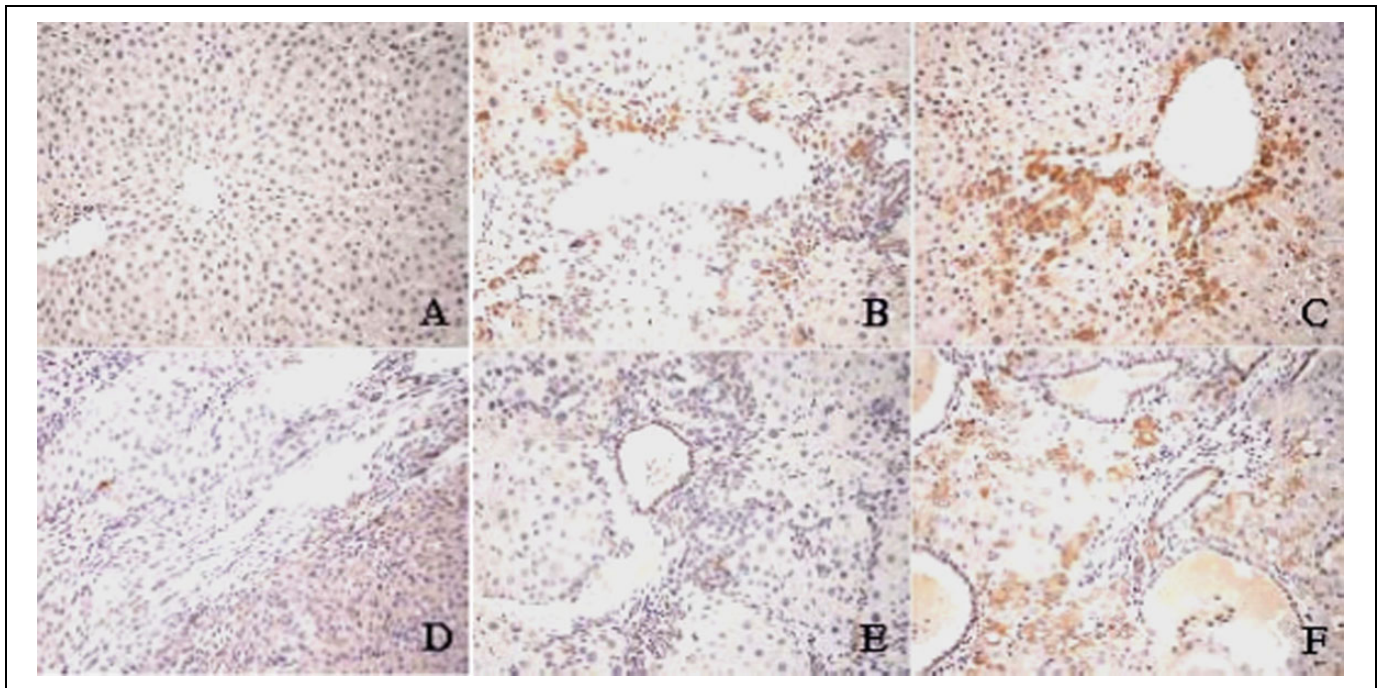


Figure 8. The location of expression of clusterin in liver tissues during induced liver cancer in rats (IHC $\times 200$). A, The expression of clusterin in the cytoplasm of hepatocytes was weakly positive in liver parenchyma at the second week. B, The expression of clusterin in the cytoplasm of hepatocytes was positive around the portal area at the fourth week. C, The expression of clusterin in the cytoplasm of hepatocytes was strongly positive around the portal area at the eighth week. D and E, The expression of clusterin in the cytoplasm of hepatocytes was weakly positive in liver parenchyma at the 14th and 18th week. F, The expression of clusterin in cytoplasm of hepatocytes was strongly positive in liver parenchyma at the 21st week.

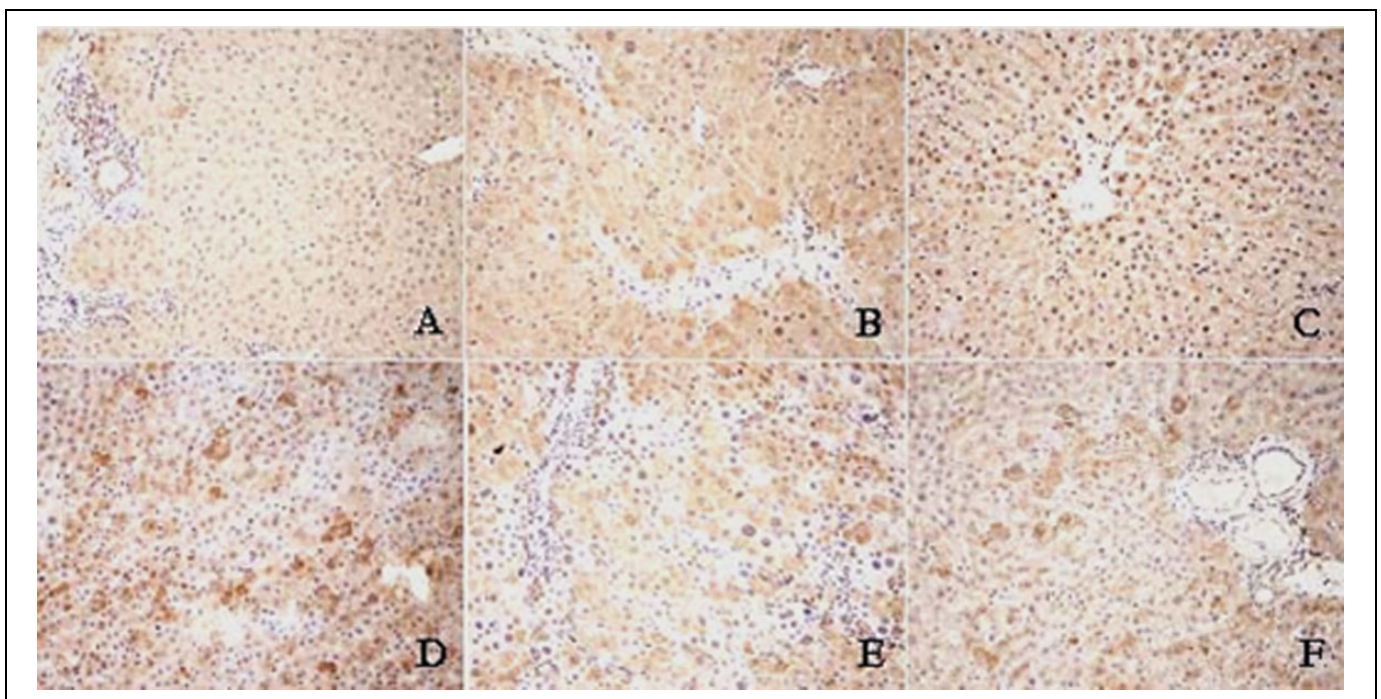


Figure 9. The location of expression of heat shock protein a8 (HSPa8) in liver tissues during induced liver cancer in rats (IHC $\times 200$). (A): The expression of HSPa8 in the cytoplasm of hepatocytes was positive in liver parenchyma at the second week. B and C, The expression of HSPa8 in the cytoplasm of hepatocytes was strongly positive in liver parenchyma at the fourth and eighth weeks. D, The expression of HSPa8 in the cytoplasm of hepatocytes was strongest positive in liver parenchyma at the 14th week. E and F, The expression of HSPa8 in cytoplasm of hepatocytes was strongly positive in liver parenchyma at the 18th and 21st weeks.

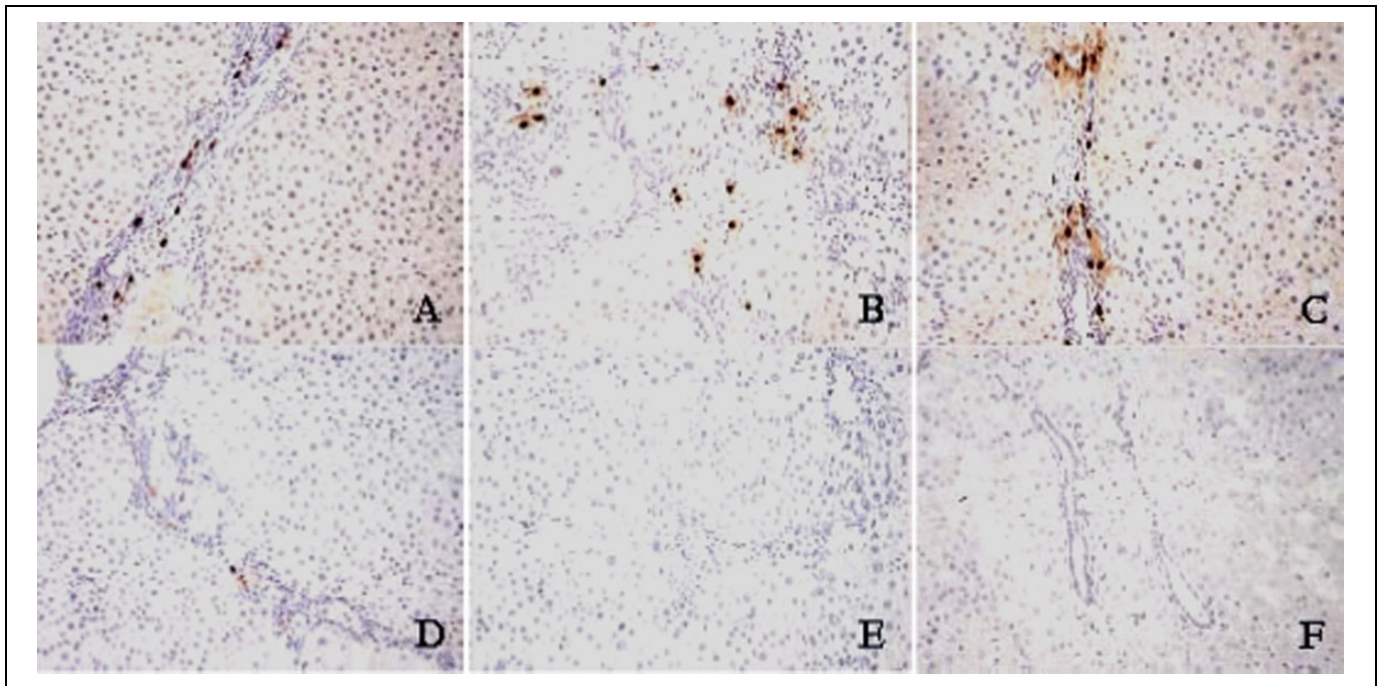


Figure 10. The location of expression of N-myc downstream-regulated gene-2 (NDRG2) in liver tissues during induced liver cancer in rats (IHC $\times 200$). A, The expression of NDRG2 in the cytoplasm and nucleus of mesenchymal cells occurred around portal area at the second week. B and C, The expression of NDRG2 in cytoplasm and nucleus of hepatocytes was strongly positive in liver parenchyma at the fourth and eighth week. D- F, The expression of NDRG2 in cytoplasm and nucleus of hepatocytes was weakly positive in liver parenchyma after the 14th week.

coordination with Bcl2, Bcl-XL, and Cr-mA. Heat shock protein $\alpha 8$ is closely related to the occurrence and development of tumor cells.^{17,18} As one of the most important subset in the HSP family, HSP70 proteins are found to be a cancer relevant survival protein. It is abundantly expressed in malignant tumors of various origins, and its expression correlates with increased cell proliferation, poor differentiation, lymph node metastases, and poor therapeutic outcome.^{19,20} The expression of HSP70 increased in lower differentiation of liver cancer cells and weak expression in mature differentiation of liver cancer cells. Moreover, the expression of HSP70 in paracancerous tissue is very weak, indicating the heterogeneity in tumor tissue differentiation because of the expression of HSP70 in cytoplasmic, nuclear, and/or cell membrane.^{21,22}

In recent years, many studies suggested that HSP70 is overexpressed in early and progressed HCC. It is believed that the specific inhibition of HSP70 expression may affect the proliferation and apoptosis of HCC cells.²³⁻²⁵ Tumor overgrowth can result in the relative insufficiency of vascular hyperplasia to induce expression of HSP70 due to hypoxia stress, it indicates that the HSP70 level may reflect the proliferation and malignant degree of HCC cells, and HSP70 is involved in early occurrence of HCC.²⁶

Our study showed that serum HSP $\alpha 8$ level gradually increased with the prolongation of time during hepatocarcinogenesis in rats. The expression of HSP $\alpha 8$ in the cytoplasm of hepatocytes was positive in hepatic parenchyma at the second week. The expression of HSP $\alpha 8$ in the cytoplasm of hepatocytes increased at the fourth and eighth week. Moreover, the

expression of HSP $\alpha 8$ in the cytoplasm of hepatocytes was persistently positive in liver parenchyma at the 21st week. The results indicated that the diethylnitrosamine agent could cause DNA and cell damage of normal liver cells; resulted in the mutation, abnormal proliferation, canceration of liver cells, and overexpression of HSP $\alpha 8$ in liver cells; and the expression level of HSP $\alpha 8$ could reflect the degree of proliferation and malignant transformation of liver cells.

N-myc down stream regulated gene 2 is a kind of gene related to cell proliferation and differentiation; participates in the occurrence, development, and prognosis of tumor; involves in hypoxia and stress reaction; and facilitates the maintenance of costimulatory signal being necessary for T lymphocyte proliferation induced by dendritic cells.²⁷⁻³⁰ N-Myc downstream-regulated gene-2 is located in the cytoplasm of cells and is involved in the cell growth and differentiation. N-Myc downstream-regulated gene-2 plays a bidirectional regulation role in liver regeneration; the NDRG2 expression decreases during early liver regeneration and promotes the division and proliferation of liver cells. However, the expression of NDRG2 increases during late liver regeneration and promotes the differentiation and maturation of liver cells.³¹ As a new candidate tumor suppressor gene, NDRG2 also plays an important role in the formation of HCC. Compared to normal and paracancerous liver tissues, the expression of NDRG2 in liver cancer tissues downregulated significantly, and the overexpression of NDRG2 was positively correlated with the differentiation of HCC. The *in vitro* experimental results showed that the expression level of NDRG2 was closely related to the proliferation,

invasion, and metastasis of liver cancer cells.^{32,33} Yang et al³⁴ found that the messenger RNA (mRNA) and protein expression of NDRG2 in hepatocytes decreased after hepatectomy for 8 hours and decreased to the lowest level at 48 hours; then, the mRNA and protein expression of NDRG2 increased gradually to the highest level after 72 hours. The positive expression rates of NDRG2 in HCC tissues and normal liver tissues were 16.67% and 100%, respectively, and the NDRG2 expression was located in the cytoplasm. The mRNA and protein expression of NDRG2 in HCC tissues was significantly lower than that in normal liver tissues, but there was no significant difference in the NDRG2 mRNA expression in different HCC tissues of Edmondson-Steiner grading. The results showed that the gene expression of NDRG2 was significantly different between HCC tissues and normal liver tissues, and NDRG2 was involved in the occurrence and development of HCC.³⁵

Our current study showed that serum NDRG2 level decreased at the 8th week, increased at the 14th week, and then decreased at the 18th week during hepatocarcinogenesis in rats. The serum NDRG2 expression was a biphasic change. The NDRG2 expression was located in cytoplasm and nucleus of mesenchymal cells around the portal area in the second week. The overexpression of NDRG2 was located in the cytoplasm and nucleus of hepatocytes in liver parenchyma at the fourth week and eighth week. The expression of NDRG2 decreased in hepatocytes at the 14th week and decreased to the lowest level at 18th week. It indicated that NDRG2 participated in the process of abnormal cell division, proliferation, and carcinogenesis of liver cells induced by diethylnitrosamine agent during hepatocarcinogenesis in rats.

So far, the exact mechanisms of the occurrence and development of HCC has not been fully elucidated. Chronic inflammation is a major driver for the transformation of genetically defective liver stem cells (LSCs) into highly metastatic liver cancer cells in premalignant liver tissue, and interleukin 6-mediated inflammation programs constitutive activation of the Transforming growth factor activated kinase1-Nuclear transcription KappaB signaling cascade in LSCs, thereby, accelerating the transformation of normal LSCs to metastatic cancer stem cells.³⁶ It is one of the research hotspots in HCC to find a new molecular and therapeutic target, which is closely related to the occurrence and development of HCC. Our present study indicates that HSPA8, clusterin, and NDRG2 participate in the process of abnormal cell division, proliferation, and carcinogenesis of liver cells during hepatocarcinogenesis, but the biological effects of the 3 proteins is not fully understood. Their structure, function, and regulating mechanism of induced activation needs further study to clarify their biological effects in different stages of the occurrence and development of HCC, and the molecular targeted drugs can be developed for these molecules. It will provide a new theoretical basis for the early diagnosis and molecular-targeted drug therapy for HCC.

In conclusion, our results indicate that HSPA8, clusterin, and NDRG2 participate in the process of abnormal cell division, proliferation, and carcinogenesis of liver cells during hepatocarcinogenesis.

Acknowledgment

We thank Dr Bolie Shu for kind help in protein mass spectrometry.

Declaration of Conflicting Interests

The author(s) declared no potential conflicts of interest with respect to the research, authorship, and/or publication of this article.

Funding

The author(s) disclosed receipt of the following financial support for the research, authorship, and/or publication of this article: This research project was supported by the major project of Science and technology commission of Shanghai Putuo district (PT2012-B-162).

References

1. Maluccio M, Covey A. Recent progress in understanding, diagnosing, and treating hepatocellular carcinoma. *CA Cancer J Clin.* 2012;62(6):394-399.
2. Jian ZX. Progress and prospect in the treatment of primary liver cancer. *J Pract Med.* 2007;23(6):773-775.
3. Ren F. Research progress of proteomics on nonmalignant liver diseases with the application of MALDI-TOF-M. *J Pract Hepatol.* 2009;12(1):59-63.
4. Shen YC, Yao DF. Evaluation of proteomics technology in early diagnosis and monitoring of Hepatocellular Carcinoma. *J Med Res.* 2008;37(9):12-15.
5. Apweiler R, Martin MJ, O'Donovan C, et al. The Universal Protein Resource(UniProt)in 2010. *Nucleic Acids Res.* 2010;38(Database issue):D142-D148.
6. Zhang Y. Application of comparative proteomics in hepatocellular carcinoma. *Int Pathol Clin Med.* 2006;27(1):40-43.
7. Paradis V, Degos F, Dargere D, et al. Identification of a new marker of hepatocellular carcinoma by serum protein profiling of patients with chronic liver diseases. *Hepatol.* 2005;41(1):40-47.
8. Hu H, Ding X, Yang Y, et al. Changes in glucose-6-phosphate dehydrogenase expression results in altered behavior of HBV-associated liver cancer cells. *Am J Physiol Gastrointest Liver Physiol.* 2014;307(6):G611-G622.
9. Alaiya AA, Franzén B, Auer G, Linder S. Cancer proteomics: from identification of novel markers to creation of artificial learning models for tumor classification. *Electrophoresis.* 2000;21(6):1210-1217.
10. Poon TC, Yip TT, Chan AT, et al. Comprehensive proteomic profiling identifies serum proteomic signatures for detection of hepatocellular carcinoma and its subtypes. *Clin Chem.* 2003;49(5):752-760.
11. Trougakos IP, Gonos ES. Clusterin/apolipoprotein J in human aging and cancer. *Int J Biochem Cell Biol.* 2002;34(11):1430-1448.
12. Qian FY, Xiong MM, Li HC, Lin ZL. Expression of clusterin in human hepatocellular carcinoma and its relationship with Caspase-3. *Chin. J Gastroenterol Hepatol.* 2009;18(7):615-617.
13. Nafee AM, Pasha HF, Abd El Aal SM, Mostafa NA. Clinical significance of serum clusterin as a biomarker for evaluating diagnosis and metastasis potential of viral-related hepatocellular carcinoma. *Clin Biochem.* 2012;45(13-14):1070-1074.

14. Li Y, Zhang QL, Yang XL, Li G, He X, Zhou Y. Clusterin is a potential serum marker of hepatic carcinoma. *Chin J Hepatol.* 2012;20 (4):275 -279.
15. Di Tommaso L, Destro A, Seok JY, et al. The application of markers (HSP70, GPC3 and GS) in liver biopsies is useful for detection of hepatocellular carcinoma. *Hepatol.* 2009;50(4):659-661.
16. Schueller G, Paolini P, Friedl J. Heat treatment of hepatocellular carcinoma cells: increased levels of heat shock proteins 70 and 90 correlate with cellular necrosis. *Anticancer Res.* 2001;21(1A): 295-300.
17. Wei YQ, Zhao X, Kariya Y, Teshigawara K, Uchida A. Inhibition of proliferation and induction of apoptosis by abrogation of heat-shock protein (HSP) 70 expression in tumor cells. *Cancer Immunol Immunother.* 1995;40(2):73-78.
18. Wu YF, Cao MF, Gao YP, et al. Down-modulation of heat shock protein 70 and up-modulation of caspase-3 during schisandrin B-induced apoptosis in human hepatoma SMMC-7721 cells. *World J Gastroenterol.* 2004; 10 (20):2944-2948.
19. Aghdassi A, Phillips P, Dudeja V, et al. Heat shock protein70 increases tumorigenicity and inhibits apoptosis in pancreatic adenocarcinoma. *Cancer Res.* 2007;67(2):616-625.
20. Wang XP, Liu GZ, Song AL, Chen RF, Li HY, Liu Y. Expression and significance of heat shock protein 70 and glucose regulated protein 94 in human esophageal carcinoma. *World J Gastroenterol.* 2005;11(3):429-432.
21. Di Cesare S, Poccia F, Mastino A, Colizzi V. Surface expressed heat - shock proteins by stressed or human immunodeficiency virus(HIV)-infected lymphoid cells represent the target for antibody-dependent cellular cytotoxicity. *Immunology.* 1992; 76(2):341-343.
22. Ralhan R, Kaur J. Differential expression of Mr 70000 heat shock protein in normal, premalignant and malignant human uterine cervix. *Clin Cancer Res.* 1995;1(10):1217-1222.
23. Chuma M, Sakamoto M, Yamazaki K, et al. Expression profiling in multistage hepatocarcinogenesis: identification of HSP70 as a molecular marker of early hepatocellular carcinoma. *Hepatology.* 2003; 37 (1):198-207.
24. Lim SO, Park SG, Yoo JH, et al. Expression of heat shock proteins (HSP27, HSP60, HSP70, HSP90, GRP78, GRP94) in hepatitis B virus-related hepatocellular carcinomas and dysplastic nodules. *World J Gastroenterol.* 2005;11(14):2072-2079.
25. Wang XP, Wang QX, Li HY, Chen RF. Heat shock protein 70 chaperoned alpha-fetoprotein in human hepatocellular carcinoma cell line BEL-7402. *World J Gastroenterol.* 2005;11(35): 5561-5564.
26. Cui Y, Dong JH, Zhou JL, Zhang M, Wu JH, Zhang JZ. Expression of HSP70 and bcl-2 in hepatocellular carcinoma and paracarcinomatous tissues. *Chin J Modern Medicine.* 2006; 16(11):1610-1613.
27. Deng Y, Yao L, Chau L, et al. N-Myc downstream-regulated gene2 (NDRG2) inhibits glioblastoma cell proliferation. *Int J Cancer.* 2003;106(6):984.
28. Park MY, Choi SC, Lee HS, et al. A quantitative analysis of N-myc downstream regulated gene 2 (NDRG2) in human tissues and cell lysates by reverse-phase protein microarray. *Clin Chim Acta.* 2008;387(1-2):84-89.
29. Choi SC, Kim KD, Kim JT, et al. Expression and regulation of NDRG2 (N-myc downstream regulated gene2) during the differentiation of dendritic cells. *FEBS Lett.* 2003;553(3):413-418.
30. Choi SC, Kim KD, Kim JT, et al. Expression of human NDRG2 by myeloid dendritic cells inhibits down-regulation of activated leukocyte cell adhesion molecule (ALCAM) and contributes to maintenance of T cell stimulatory activity. *J Leukoc Biol.* 2008; 83(1):89-98.
31. Yang J, Li Y, Wu L, et al. NDRG2 in rat liver regeneration: role in proliferation and apoptosis. *Wound Repair Regen.* 2010;18(5): 524-531.
32. Shon SK, Kim A, Kim JY, Kim KI, Yang Y, Lim JS. Bone morphogenetic protein-4 induced by NDRG2 expression inhibits MMP-9 activity in breast cancer cells. *Biochem Biophys Res Commun.* 2009;385(2):198-203.
33. Lee DC, Kang YK, Kim WH, et al. Functional and clinical evidence for NDRG2 as a candidate suppressor of liver cancer metastasis. *Cancer Res.* 2008;68(11):4210-4220.
34. Yang JD, Li Y, Tao KS, et al. The mechanism of NDRG2 regulating the liver regeneration in the rats. *Chin. J Gastroenterol Hepatol.* 2010;19(5):440-443.
35. Wu GQ, Zhang J, Li KZ, Dou KF, Liu XP. The expression and significance of NDRG2 gene in primary hepatocellular carcinoma and normal hepatic tissues. *Chin J Bases Clinics In General Surgery.* 2012;19(3):266-270.
36. Mitra A, Yan J, Xia X, et al. IL6-mediated inflammatory loop reprograms normal to epithelial-mesenchymal transition+ metastatic cancer stem cells in preneoplastic liver of transforming growth factor beta-deficient β 2-spectrin \pm mice. *Hepatol.* 2017;65(4):1222-1236.
37. Ma Y, Hua YP, Chen ZB, Zhang JX. Induction of chemical hepatocarcinogenesis and establishment of orthotopic liver transplantation model with hepatocarcinoma in rats. *National Medical J Chin.* 2006;86(12):850-853.
38. Bradford MM. A rapid and sensitive method for the quantitation of microgram quantities of protein utilizing the principle of protein-dye binding. *Anal Biochem.* 1976;72(7):248-254.